

Analysis on structural and thermal properties of BeO nanoparticles and filled polymer matrix

M. F. Nabihah & S. Shanmugan

disis_mi@yahoo.com, subashanmugan@gmail.com

School of Physics, Universiti Sains Malaysia (USM), 11800, Minden, Pulau Pinang, Malaysia

Corresponding author: Tel:+60-04-6533672; Fax: +60-04-6579150;

e-mail: subashanmugan@gmail.com

Abstract:

Beryllium oxide (BeO) nanoparticles were synthesized by polyacrylamide gel route and various calcination temperature was applied during the synthesis process. The synthesized BeO nanocrystallites were examined by x-ray diffraction (XRD), scanning electron microscope (SEM), thermogravimetric analysis (TGA) and Transient Plane Source (TPS) Analysis. Structural parameters such as lattice parameter, lattice constant and were calculated using the XRD results. The size of the BeO crystallites were calculated by X-ray diffraction (XRD) which is 49.25 nm for sample calcined at 800°C and that was the lowest one. SEM analysis also shows an almost same value of size particles with XRD result for all sample. It also depicts an irregular shape for all sample. The calcination temperature applied on the BeO powder and the amount of filler added does affect the thermal conductivity of BeO filled epoxy which is favourable for thermal interface material (TIM) application in LED packages. Thermal conductivity composite become higher when the particles size increase within the same volume of fraction. The filler loading does effect the epoxy composition in term of thermal diffusivity and the result for specific heat capacity did show an increasing trend when more filler was added.

Keywords

BeO, Nano Particles, Polyacrylamide gel route, Structural Parameters, XRD analysis, TGA analysis, TPS analysis, SEM analysis.

1. Introduction

Light emitting diodes (LED) have attracted a great deal of attention from the lighting industry as it holds a promising characteristic of being versatile

and environmentally friendly [1]. The energy efficiency of LED also has been improved a lot and make the technology growing faster in sectors of enabling new lighting systems [2]. Only 20-30% of LED's electric power were converted into visible light, the rest will convert into a heat [3]. Thus, it is essential for the heat generated at the device to be dissipated as effectively as possible. However, the interface problem exists with the LED package. Therefore, thermal interface materials (TIMs) as crucial components of advanced high density electronic packaging are needed in the system in order to obtain a good heat dissipation. Thus, it will prevent the failure of electronic components due to overheating [4].

Recently, ceramic particles filled polymer as material of TIM have become a trend as it offers a good thermal conduction with low electrical conductivity. Several materials for ceramic composites have been introduced such as magnesium oxide (MgO), aluminium nitride, boron nitride, silicon carbide and beryllium oxide (BeO) [5]. Then, BeO ceramics have been chosen as the best one as it possesses high thermal conductivity, high melting point, high intensity, high insulation nature, high chemical and thermal stability, low dielectric constant, low dielectric loss and good technology applicability [6].

Few methods have been reported for the synthesis of nanoparticles such as the sol gel method, high energy ball milling and the polyacrylamide gel route [7]. Nowadays, polyacrylamide gel route is the preferred method to synthesize nanoparticles of a variety of oxide materials [7]. This polyacrylamide gel technique offers a highly time-saving manner with a simple, convenient and inexpensive synthesizing process. It also need a relatively lower calcination temperature than traditional preparation technique [8].

In the past decade, a wide range of combination of polymers and conductive fillers were prepared to form composites exhibiting useful properties as TIM.

Polymers can be easily made into polymer matrix composites as it has low processing temperatures [9]. Epoxy resin has been chosen as the polymer in this research. In the present work, BeO nanoparticles were synthesized by polyacrylamide gel method. The role of calcination temperature on the size, intensity peaks, morphology, decomposition temperature of material and other structural parameters of BeO nanoparticles have been examined in this study. Moreover, thermal properties of BeO filled epoxy resin also have been studied with addition of different percentages of filler.

2. Experimental

2.1. Synthesis of Beo nanoparticles

Beryllium Oxide nanoparticles were synthesized by polyacrylamide gel method. Beryllium sulfate tetrahydrate ($\text{BeSO}_4 \cdot 4\text{H}_2\text{O}$), Acrylamide (AM) and N, N'-Methylene-bis-acrylamide (MBAM) were used as the starting material. An experimental procedure of polyacrylamide gel route for preparing BeO nanoparticles is as follows. Firstly, beryllium sulfate tetrahydrate was dissolved in the distilled water with moment stirring to produce a transparent 1.5 mol/L BeSO_4 solution. 5 wt% organic agents AM and MBAM monomers with a mass ratio of 20 were added in the prepared solution with constant stirring until the solution became transparent. Then, 0.5 mL ammonium persulfate solution (ASP: 10 wt%) was added as initiator and the temperature of the solution was increased slowly to 60°C in water bath.

The initiator APS initiated the free-radical crosslinking copolymerization of AM and MBAM. The mixture was turned to transparent hydrogel gradually. The condition was held for 1 hr in order to make sure that organic onomers react absolutely. Then, the gel was dried at 80°C for 48 hr in a vacuum oven. The formed xerogel was homogenized in a ceramic mortar and calcined at various temperatures (800 °C, 900 °C and 1000°C) with a laboratory furnace in the presence of air at a heating rate of 5 °C/min. It is to obtain nanoparticles of a pure BeO phase.

2.2 Composite preparation

BeO filled epoxy resin was prepared by mixing calcined BeO powder with the epoxy polymer solution using homogenizer equipment (Make: Kakuhunter Homogenizer, Model:SK-300S) in order to get good dispersion into polymer solution and prevent bubble forming. The said equipment was rented from M/s Gaia Science Sdn Bhd., to prepare the homogenised epoxy resin. The total weight of the mixture (epoxy and filler) is fixed as constant as 20g

for each sample. Novolac resin polymer was purchased from Orient Technology Sdn. Bhd and used to mix with the synthesized BeO powder. The resin was conditioned by mixing some chemicals. Mixture of 20g of the BeO filled epoxy was carried out by mixing 0.1g and 0.2 g of BeO powder with 19.9 g and 19.8 g of epoxy resin mixture.

The epoxy mixture was prepared by two part of system (A and B). In Part A, it consists of neat novolac epoxy resin. In Part B, it consists of the mixture of Methylhexahydrophthalic anhydride (MHHPA) and 1-Methylimidazole. MHHPA will act as hardener and need to be used in sufficient amount to cure the epoxy composition while 1-Methylimidazole is a curing catalyst that accelerates a curing reaction between the epoxy resin and a hardener [10]. Uncured epoxy resins have only poor mechanical, chemical and heat resistance properties. However, good properties can be obtained by curing process and curing may be achieved by forming a copolymer with hardeners. So part B was poured into part A and mixed for 10 minutes by the homogenizer so that the mixture is well incorporated with the other.

Total mass of the mixture prepared in this experiment were approximately 19.9g and 19.8 g, with the ratio of the composition is 100:85:1 for resin: MHHPA : catalyst. The amount of the epoxy resin in the epoxy composition is desirably 95 wt % or less based upon the total weight of the epoxy composition. The weight content of the curing catalyst is preferably 1% or less, based upon the total weight of the epoxy composition. The content of the fillers is desirably 20% by weight or more based on the total weight of the filled epoxy [11].

2.3 Characterization

X-ray powder diffraction (XRD) analysis have been carried out by X-ray diffractometry (XRD-Siemens diffractometer D5000). It is to study the microstructure, phase analysis and structural parameters of BeO nanoparticles calcined at various temperatures of 800 °C, 900 °C and 1000 °C. Structural parameters such as lattice parameter, lattice constant, volume of cell and crystallite size were also calculated using the XRD results. Scanning Electron Microscope (SEM) analysis was conducted to determine the surface morphology and composition of BeO nanoparticles calcined at various temperatures of 800 °C, 900 °C and 1000 °C. The size of particles also can be estimated from this analysis. Thermogravimetric analysis (TGA) was performed using Perkin Elmer Diamond in N_2 atmosphere at temperature range of 25 – 1000 °C with scanning rate of 5°C/min. The weight of all samples was in the range of 11–13 mg. All samples of BeO (800 °C, 900 °C and 1000°C) were tested by

TGA in order to identify the exact decomposition temperature of the material. Next, Thermal Constant Analyser TPS 2500 S was used to determine the thermal conductivity of BeO powder filled epoxy resin at 25°C with variation of heating power from 20 to 30 mW and the test time from 20 to 40s based on the sample compatibility.

3. Result And Discussion

3.1. Xrd Analysis

Figure (1-3) represents the X-ray powder diffraction (XRD) patterns of the synthesized BeO nanoparticles powder obtained by polyacrylamide gel route calcined at various temperatures (800 °C, 900 °C and 1000 °C). The diffraction pattern of all samples is in well agreement with the data of JCPDS File No. [78-1379] with characteristic of hexagonal pattern with lattice constants of $a=2.6990$ and $c=4.3850$. All peaks are indexed using the XRD software and clearly show the variation of intensity of preferred orientations with respect to the calcination temperatures. The pattern in fig (1-3) show three sharp and well defined diffraction lines related to (100), (002), and (101) orientation of BeO nanoparticles. Moreover, the well-defined intense peaks of the above phases in diffraction pattern indicate that the synthesized BeO nanoparticles have preferred growth on these orientations than other planes with excellent crystallinity.

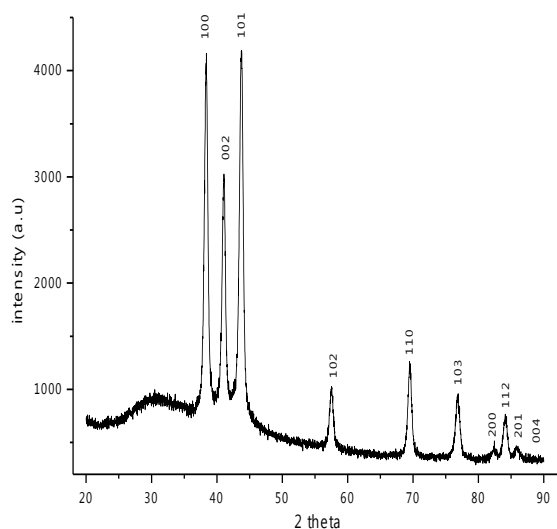


Fig 1. XRD patterns for BeO nanoparticles powder calcined at 800 °C for 2 hr.

Fig. 4 (a-c) shows a significant difference in the intensity of the peak observed from the BeO samples calcined at 800 °C, 900°C and 1000 °C for their preferred orientations [(100), (002), and (101)]. The pattern of the graph is anomalous as it is increasing linearly when the temperature increasing. In fig. 4, it is clearly indicating that the highest intensity for all orientations is observed for the samples calcined at 800 °C followed by 1000 °C and 900 °C. Even the sample calcined at 800 °C depicts the highest diffraction intensity which is opposites from the result obtained by Wang et al. [7] but the peaks for the sample still depicts a broader width than sample at 1000 °C as can be observed in fig. 4.

However, it is shown that the sample at 900 °C exhibits a broadest peak followed by 800 °C and 1000 °C. The broader the width of the diffraction peak, the smaller the size which is in good agreement with the result obtained in the table 1. It is because the size obtained at 002 orientation for sample at 900 °C have the smallest size at 19.15 nm but still when we observed it from the average size of the sample, 800 °C still got the smallest crystallite size among them. Hence, the sample calcined at 800 °C is the one that exhibit the most excellent crystallinity. As shown in fig. 4, the highest intensity was noticed with (101) orientation compared to other orientations for all calcined temperatures which is suggesting a preferential orientation of the crystals along the a and c axes and a good crystallization of the synthesized BeO nanocrystal [11,12].

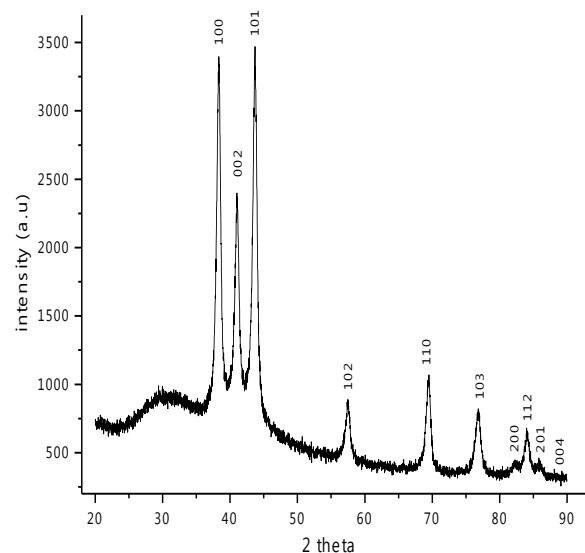


Fig 2. XRD patterns for BeO nanoparticles powder calcined at 900 °C for 2 hr.

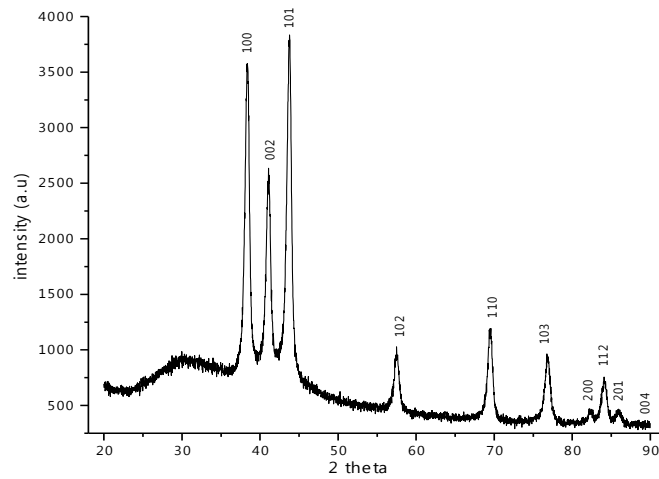


Fig 3. XRD patterns for BeO nanoparticles powder calcined at 1000 °C for 2 hr.

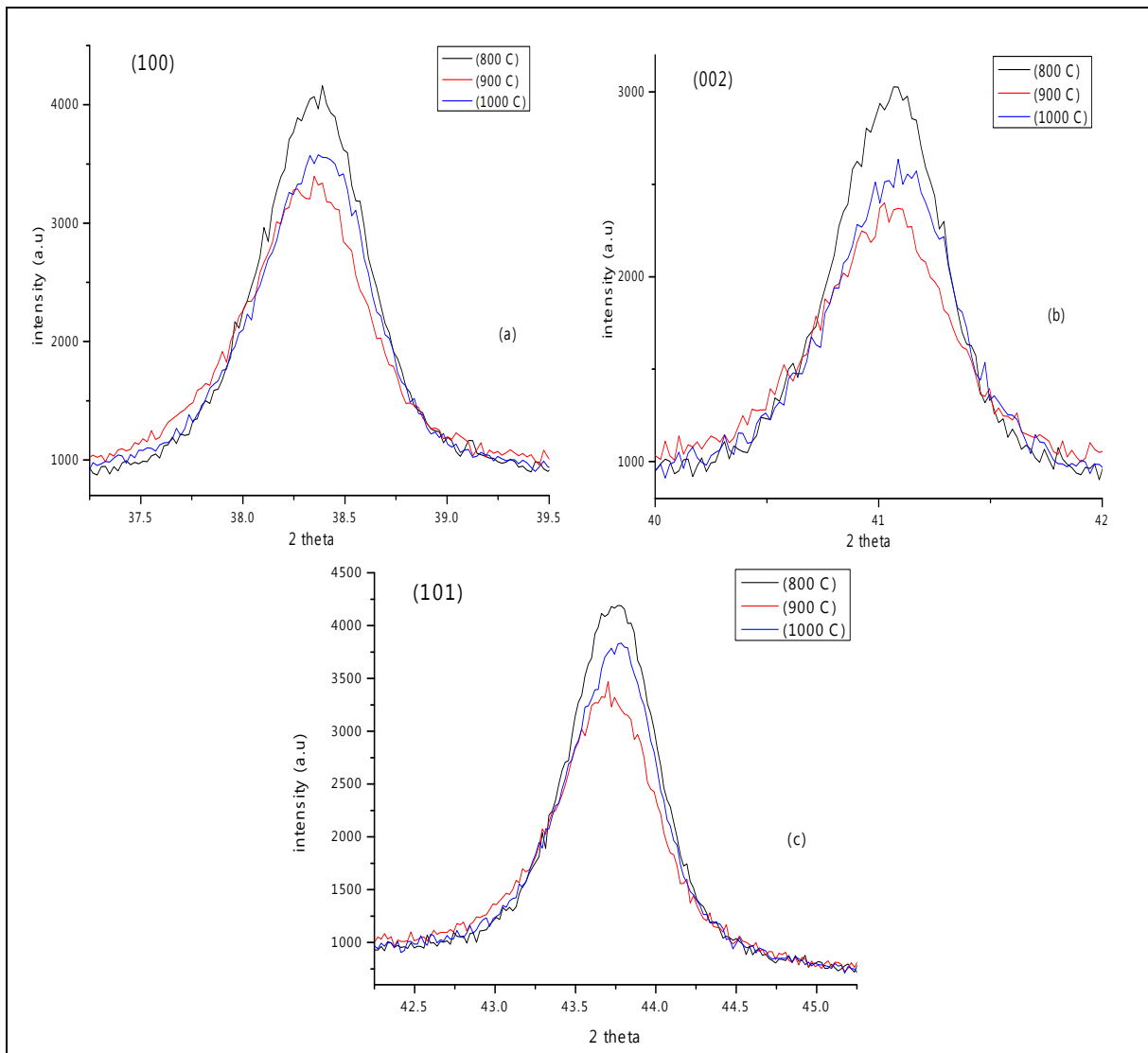


Fig 4. XRD patterns of (100), (002) & (101) oriented peaks of BeO phase calcined at various temperature for 2 hr.

From the XRD data, some of the structural parameter of BeO nanoparticles have been measured and shown in Table 1 below. Firstly, the particle size, D of the BeO nanoparticles was calculated by using the Debye-Scherer equation [13]:

$$D = k\lambda / \beta \cos \theta \quad (1)$$

where D is in the nano range, $\lambda = 1.5406 \text{ \AA}$ is the wavelength of the radiation used, $k = 0.94$ is a constant, β is full width half maximum (FWHM) in radian and θ is the Bragg diffraction angle of the XRD peak. 3 dominant peaks of $\{(100), (002) \&$

$(101)\}$ were calculated for its crystallite size for all of the sample. The measurement depicts that the average size of the crystallite sizes of the synthesized powders for sample calcined at $800 \text{ }^\circ\text{C}$ is 49.25nm while 61.37nm for $900 \text{ }^\circ\text{C}$ and 71.01 nm for $1000 \text{ }^\circ\text{C}$. Here, it proved that all of the sample were categorized as a nanoparticle as the size is lower than 100 nm .

Table 1. Structural parameter of BeO nanoparticles calcined at various temperature for 2 hr.

Calcination temperature, ($^\circ\text{C}$)	Orientation, (hkl)	Lattice constant, ($\times 10^{-10}$)		Crystallite size, D (nm)	Lattice parameter, ($\times 10^{-10}$)	Volume of cell, ($\times 10^{-10}$) ³
		a	c			
800	(100)	2.7024	4.6807	52.83	2.3403	29.6025
	(002)	2.5334	4.3880	42.08	2.1940	24.3889
	(101)	2.3822	4.1261	52.83	1.8453	20.2775
900	(100)	2.7055	4.6861	104.9	2.3430	29.7047
	(002)	2.5340	4.3890	19.15	2.1945	24.4060
	(101)	2.3786	4.1199	60.07	1.8424	20.1859
1000	(100)	2.6984	4.6738	69.26	2.3369	29.4714
	(002)	2.5286	4.3797	86.17	2.1899	24.2506
	(101)	2.3836	4.1285	57.61	1.8463	20.3131

$$c = \lambda / \sin \theta \quad (4)$$

The broadening of the diffractions peaks is related to the crystallite size as the size became smaller, the diffractions peaks will be broadened more [14]. Mechanical, electrical, thermal, optical and chemical properties of particles will change to a better property when the particle size of filler becomes smaller to nanometric level [15]. Hence, this sample is suitable to become the filler for the next experiment.

From the table above, the calculated results show that the size increased as the calcined temperature rises, which is in a good agreement with reported work by Wang et al. [7]. The smaller size can be seen in most of the (002) orientation in all of the sample. However, the sizes displayed at (101) orientation for all of the sample are the most likely to each other as the highest peaks of intensity for all of the sample were also at (101) orientation.

Lattice parameter can be obtained using equation (2) and it is related with lattice constant with equation of (3) and (4) as below [16]:

$$d_{hkl} = 1 / \sqrt{[(4(h^2+k^2+hk)/3a^2) + (l^2/c^2)]} \quad (2)$$

$$a = \lambda / (\sqrt{3} \sin \theta) \quad (3)$$

where d is the interplanar distance, λ is the wavelength 1.5406 \AA , θ is the Bragg angle. Expansion of the crystal lattice depends on the change in lattice parameters [17]. Based on the table 1 above, the values of lattice constant of all of the orientation for all of the sample were in the same range. Thus, the lattice parameter for all of it was almost constant to each other. The highest value of lattice parameter seems to be at (100) orientation and the lowest one at (101) orientation.

Moreover, the cell volume is anticipated since there is a change in lattice parameters. Volume cell, V was calculated by using the following relation [18]:

$$V = 0.866 a^2c \quad (5)$$

The calculated average values are given in the same table 1. The results show that the volume cell for all of the sample were almost same. The highest value of volume cell for sample calcined at $800 \text{ }^\circ\text{C}$, $900 \text{ }^\circ\text{C}$ and $1000 \text{ }^\circ\text{C}$ was at (100) orientation while the lowest value obtained was at (101) orientation. However, all of the value in the orientation obtained was in the range of $\sim 20 \text{ \AA}^3$.

$$(3)$$

3.2. Thermogravimetric analysis (TGA)

Thermogravimetric Analysis measures weight/mass change (loss or gain) and their rate of change as a function of temperature, time and atmosphere of the materials during the process. Since BeO is suggested for thermal interface material application as filler and their material weight loss behaviour should be addressed. Therefore, TGA was performed on the calcined BeO powder at three different temperatures as shown in fig.5. A noticeable change in TG curves could be noticed for all samples as presented in Fig. 5. In order to identify the exact decomposition temperature of the material, the analysis was done for a wide temperature range from 25 to 1000 °C at the heating rate of 5°C/min.

It was observed from the Fig. 5 (a) that a slight weight loss was occurred initially between 25 °C to 100 °C which corresponds to the evaporation of water molecules and volatile organic substances as much as 0.7 % in our samples. When further heated up to 812 °C and reach the onset, it is observed that the material loss or decomposition of material content in the powder upto this temperature is gradually decreasing as much as 1.5 %. The residue left after that is 97.8 %. Then, at ~812°C, a significant weight loss of about 2.6 % was observed. The remaining residues of the powder itself as much as 95.2% was observed at 1013 °C.

Besides that, the pattern of the graph for the samples calcined at 900 and 1000°C as shown in Fig. 5(b) and (c) were slightly different from the Fig. 5(a) because of the difference in buoyancy due to the slight change in the density of the sample [19]. From the pattern of Fig. 5(a), it depicts that most of the moisture escaped on the melting process [19]. For both Fig. 5 (b) and (c), a noticeable weight loss (~4.5%) and (~2.9 %) were observed in between 25 °C and 100 °C. An irregularity in weight loss from 100 °C to 1000 °C can be seen from two temperatures (900 °C and 1000 °C) as presented in Fig. 5 (b) and (c). The residues at the end of the analysis was differ for each calcination temperatures which is 89.9 % for sample calcined at 900 °C while 93 % for sample calcined at 1000 °C. However, it can be easily interpreted from the TG curves of samples that the remaining weight did not level off even near to 1000 °C and there was no weight lost above approximately 1000 °C for all sample.

Moreover, there are still a lots of weight percentages of remaining residues of the powder itself for all of the sample can be seen in the Fig. 5. That shows that this synthesized BeO nanoparticles powder can withstand the high heat imposed on it quite stably and the contents mostly from the pure of beryllium oxide elements. It depicts that this method of synthesizing of BeO nanoparticles was a

successful one as it produces a huge amount of pure BeO nanoparticles.

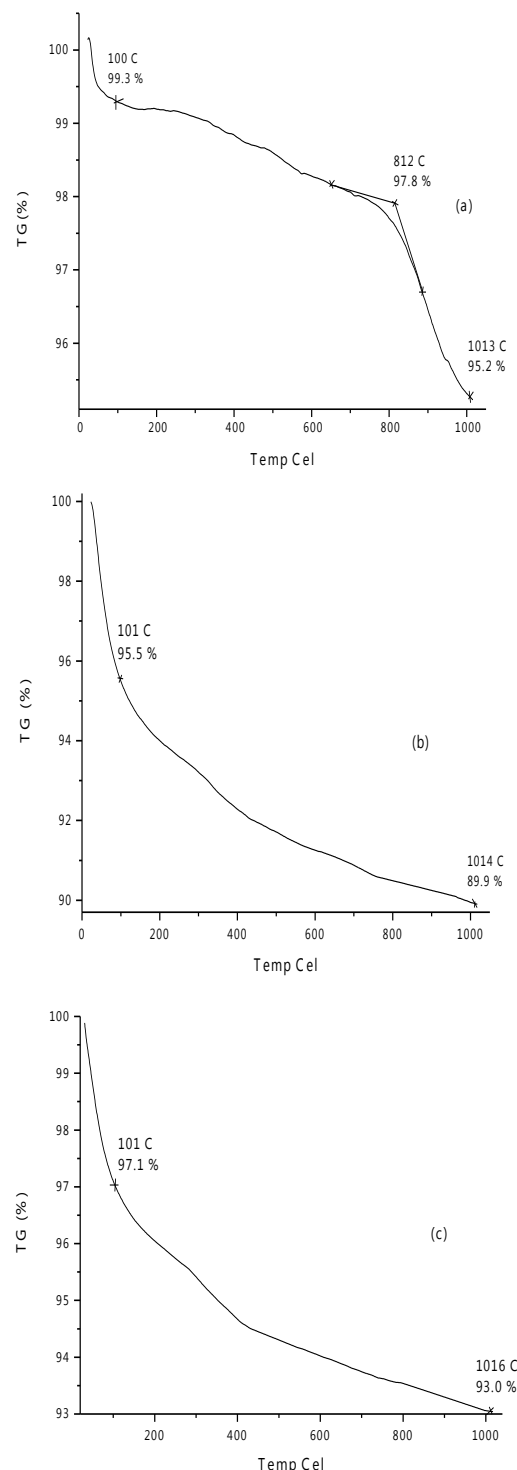
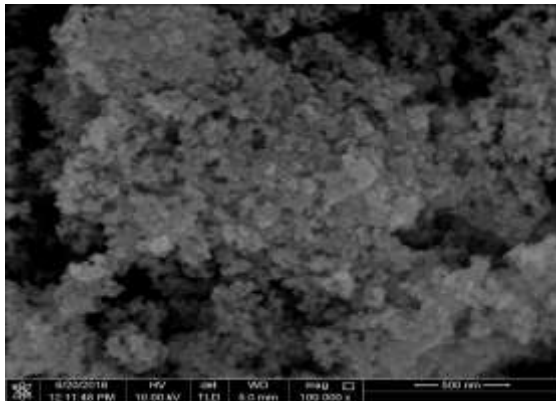
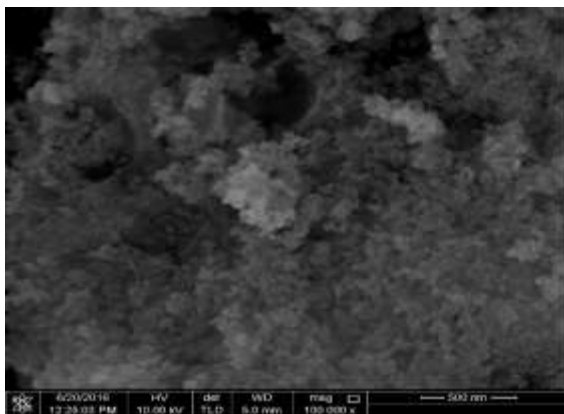


Figure 5. Thermogravimetric analysis of BeO powder with different calcination temperature; a) 800 °C b) 900 °C c) 1000 °C.

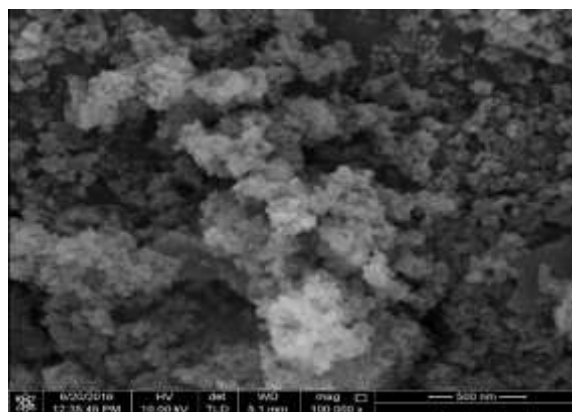
3.3. Sem Analysis



(a) 800 °C



(b) 900 C



(c) 1000 C

Figure 6. SEM micrograph of various synthesized BeO powder that have been under different calcination temperature of (a) 800 °C, (b) 900 °C and (c) 1000 °C for 2 hr.

The surface morphology of synthesized BeO nanoparticles were characterized by SEM analysis and observed agglomerated nanoparticles with average particles size of about 100 nm. In fig. 6 (a-

c), the crystallite size of all samples estimated from the SEM analysis was nearly same from the results observed by the XRD results. As expected, the sizes of nano particles are also increased when the calcined temperature is increased. As we can see from the fig.6 that the observed particles are having irregular shape for all samples. The samples calcined at 800 °C and 900°C are showing dense structure than calcined at 1000°C with cluster surface. Besides that, the particles of sample calcined at 800 °C in Fig. 6(a) agglomerated more than the other two samples and mostly the formation of the agglomeration in a ceramic powder is because of the diffusion bond formed during calcination [20]. However, from Fig. 6(c), the cluster particles make the measurement size of the particle in the sample becomes bigger.

3.4. Transient Plane Source (TPS) Analysis

Table 2. Thermal conductivity of neat epoxy.

Neat Epoxy

Percentage of filler, %	Thermal conductivity, W/mK	Thermal Diffusivity, mm ² /s	Specific Heat Capacity, MJ/m ³ K
0	0.1475	0.07597	1.942

Table 3. Thermal conductivity of Beo filled epoxy with different of calcined temperature and percentages of filler.

Epoxy + BeO (filler)

Percentages of filler, %	Temperature, °C	Thermal conductivity, W/mK	Thermal Diffusivity, mm ² /s	Specific Heat Capacity, MJ/m ³ K
0.5 (0.1g)	800	0.1483	0.07745	1.914
	900	0.1495	0.08026	1.863
	1000	0.1506	0.07818	1.927
1 (0.2g)	800	0.1498	0.07931	1.889
	900	0.1517	0.07806	1.944
	1000	0.1525	0.07852	1.942

Table 2 shows thermal conductivity of neat epoxy while table 3 depicts the thermal conductivity

of BeO filled epoxy along with thermal diffusivity and specific heat capacity of all samples for two BeO concentrations in the epoxy. In order to understand the effect of small quantity of BeO nano particles on thermal conductivity of neat epoxy, 0.1g and 0.2g of BeO nano powder mixed neat epoxy are used in this analysis. Thermal conductivity is the time rate of steady heat flow through unit thickness of an infinite slab of homogeneous material induced by unit temperature difference in a direction perpendicular to the surface. The working temperature levels of a material was determined by its property [21]. The thermal conductivity of neat epoxy resin obtained from this experiment is 0.1475 W/mK which is doubled the amount of 0.06 W/mK obtained by Roland et al. [22].

The smaller the sizes of particles is better for a filler because nano-sized of a filler possessed a higher specific surface area than the micron-sized and will affected in a greater interfacial contact area. Besides that, number particles for the nano filler is higher than the micron one for the same volume fraction of filler added and the interparticle distance of the nano filler also will be smaller [23]. However, when the particles size were already in the nano-range and also in the same volume fraction, the bigger the size is better. That's why from table – 3, the thermal conductivity of the BeO powder filled epoxy increased as the calcination temperature of BeO powder increased from 800 to 1000 °C. It is because the composite's thermal conductivity would be higher when the particles size increase within the same volume of fraction (~1000 °C is the highest one) [24,25], but still the range size of this BeO nanoparticles obtained in this research were not differs too much with each other due to the limited small amount of volume fraction added. Hence, the thermal conductivity of the composites for the sample with the 1000 °C calcined BeO filler was also not differs too much from the other two sample.

In addition, thermal conductivity is also increased when the filler content increased to the neat epoxy resin. The increment rate is low when compared with the published work by Roland et al. [22]. The increase of the thermal conductivity (300 W/mK) is apparently due to that the thermal conductivity of the filler is much higher than that of the matrix (0.1475 W/mK for epoxy resin) [26]. Overall, it shows that the calcination temperature applied on the BeO powder after synthesis and the amount of filler added are affected the thermal conductivity of BeO filled epoxy resin. It is concluded that the calcined temperature for prepared BeO nano particles will increase the performances of BeO filled epoxy which is favourable for thermal interface material (TIM) application in LED packages.

Besides that, the thermal diffusivity data that were obtained at 0.5 and 1 % filler loading were

shown in both of table 2 and 3. Thermal diffusivity of polymer material is usually specified to determine their ability to transfer heat. It is related to thermal conductivity, density and specific heat capacity [21]. From table -2, the thermal diffusivity of neat epoxy obtained from the analysis is only 0.07597 mm²/s. Meanwhile in table -3, we can see that within the same percentages loading of filler (0.5 %), the sample with the 900 °C calcined BeO filler achieves the highest thermal diffusivity of 0.08026 mm²/s before dropping slightly to 0.07818 mm²/s at the sample with the 1000 °C calcined BeO filler.

Meanwhile, at 1 % loading of filler, the sample achieved a maximum diffusivity of 0.07931 mm²/s at the sample with the 800 °C calcined BeO filler. After obtained the highest value at sample with a filler calcined at 800°C, a slightly continuous drop is observed for the sample with the filler calcined at 900 °C and 1000 °C which is 0.07806 mm²/s and 0.07852 mm²/s respectively. Hence, even though the analysis shows an irregular value of thermal diffusivity with the increment of percentages loading of filler and temperature, the filler loading still effect the epoxy composition in term of thermal diffusivity even just a little bit of change as can be seen in both of the table above. So this material is suitable as a TIM because higher thermal diffusivity values will make the composite materials transport heat more rapidly and causing them to cool more quickly so that the processing time cycles become shorter [27]. However, maybe this types of composites need a high filler loading over 10 %, so that it can exhibit more of increased changes in the thermal diffusivity compared with the composites with low filler loading like this [28].

Furthermore, as can be observed in table-3, when the values of specific heat capacity increase, the thermal diffusivity of sample will be decreased and vice versa as both of it related to each other by equation [21]:

$$\alpha = k / (\rho C_p) \quad (6)$$

where, α is thermal diffusivity in m²·s⁻¹, k is thermal conductivity in W·m⁻¹·K⁻¹, ρ is density in kg·m⁻³ and C_p is specific heat capacity in J·kg⁻¹·K⁻¹ but then the unit of C_p has been change to MJ·m⁻³·K⁻¹. Next, thermodynamic quantity that determines the amount of heat necessary to raise by one degree the temperature of a unit mass of material was known as specific heat capacity [29]. The values obtained from neat epoxy and after loaded with filler were irregular and does not change much with increment of temperature and filler loading while Jasper et al.[21] stated that generally, specific heat capacity increased when the temperature increased. This is maybe due to the limited and small amounts of filler loaded in the epoxy composition. However, it still reaches a maximum of 1.944MJ/m³K at 1 % loading at the sample with the 900 °C calcined BeO filler and

that shows that the value does increase a bit when the filler was added. Besides that, as can be seen in table -3, the results still did show an increasing trend when more filler was loaded because the values obtained at 1 % loading were a little bit higher than at 5 % loading.

4. Conclusion

BeO nanoparticle powders have been successfully synthesized by polyacrylamide gel route. The sample calcined at 800 °C is the one that exhibit the most excellent crystallinity. The measurement depicts that the lowest average size of the crystallite sizes of the synthesized powders is when the sample calcined at 800 °C which is 49.25 nm. All of the volume cell in the orientation obtained was in the range of $\sim 20 \text{ \AA}^3$. The sizes in the SEM images also increased when the calcined temperature increased. Most of the particles in all of the SEM image are irregular in shape. The calcination temperature applied on the BeO powder and the amount of filler added does affect the thermal conductivity of BeO filled epoxy. The composite's thermal conductivity increases with the particles size within the same volume of fraction. The filler loading does effect the epoxy composition in term of thermal diffusivity and specific heat capacity.

5. Acknowledgements

This research is fully supported by USM Short Term Grant (304/PFIZIK/6313160). The Kakuhunter Homogenizer, Model:SK-300S equipment was rented from M/s Gaia Science Sdn Bhd., and used to prepare the homogenised epoxy resin.

6. References

- [1] C.H. Chao Chen, L.J. Yu, C.H. Yi, *Opt. Express*, 21, 2013, 3.
- [2] LED Professional Review, 2, Luger Research & LED professional, June 2007.
- [3] Curran, Dr. John W. n.d. "Understanding LED Technology, Part 2: The Limitations of LED Lighting." *Philips*, <http://www.sitelighting.com/index.cfm>.
- [4] Schelling P. K., Shi L. & Goodson K. E. Managing heat for electronics. *Mater. Today* 8, 2005, 30–35
- [5] A. F. Z. Han, *Prog. Polym. Sci.* 36, 2010, 914.
- [6] Akishin G P, Turnaev S K, Vaispapur V Y, Gorbunova M A, Makurin Y N, Kiiko V S, Ivanovskii A L., "Thermal conductivity of beryllium oxide ceramic" [J]. *Refractories and Industrial Ceramics*, 50(6), 2009, 465–468.
- [7] Xiaofeng Wang, Richu Wang, Chaoqun Peng, Tingting Li and Bing Liu. 27(2). "Growth of BeO Nanograins Synthesized by Polyacrylamide Gel Route." *J. Mater. Sci. Technol*, 2011, pp. 147-152.
- [8] M. Tahmasebpour, A.A. Babaluo and M.K. Razavi Aghjeh, *J. Eur. Ceram. Soc.*, 28, 2008, 773.
- [9] P. Anithambigai, D. Mutharasu, L. H. Huong, T. Zahner, D. Lacey, "Synthesis and thermal analysis of aluminium nitride filled epoxy composites and its effective application as thermal interface material for LED applications", *J Mater Sci: Mater Electron*, 17 August 2014, DOI 10.1007/s10854-014-2238-y.
- [10] Tong Ping T. Xiu, Yong-Jiang Li, Hongyu Chen, Yi Zhang, Ming L. Ji, "Functional silane-compatible epoxy compositions for insulation applications" *Patent US9127116 B2*. 30 Dec 2011.
- [11] Q.A.H. Al-Naser et al., "ZnO single crystal microtubes: Synthesis, growth mechanism, and geometric structure using direct microwave." *Ceramics International* 42, 2016, 828–833, DOI: 10.13140/RG.2.1.2775.2400.
- [12] Hyoun Woo Kim, Nam Ho Kim, Chongmu Lee, "Very Low Temperature Growth of ZnO Thin Films on Si Substrates Using the Metalorganic Chemical Vapor Deposition Technique." *Journal of the Korean Physical Society*, Vol. 44, No. 1, January 2004, pp. 14-17.
- [13] P. R. Parmar, M. H. Mangrola, B. H. Parmar, and V. G. Joshi, *Multi Disciplinary Edu. Global Quest*. 1, 2012, 146.
- [14] T. Theivasanthi* and M. Alagar, "Electrolytic Synthesis and Characterizations of Silver Nanopowder".
- [15] Berkan EMEK, "A Study On Thermophysical Properties Of Graphite Filled Polymer Nanocomposites", February 2013, pp 34-42.
- [16] M.A. Gondal, Q.A. Drmosh, Z.H. Yamani, T.A. Saleh, "Synthesis of ZnO nanoparticles by laser ablation in liquid and their annealing transformation into ZnO nanoparticles", *Appl. Surf. Sci.* vol. 256, Oct. 2009, pp. 298 – 304.
- [17] P. Singh, A. Kumar, Deepak, D. Kaur, "ZnO nanocrystalline powder synthesized by ultrasonic mistchemical vapour deposition", *Opt. Mater.* vol. 30, April 2008, pp. 1316 – 1322.
- [18] B. Gopal Krishna, M. Jagannadha Rao, "Biosynthesis and measurement of thermal conductivity of ZnO material", *International Journal of Engineering Trends and Technology*, vol. 26(5), Aug 2015, pp. 272-275.
- [19] www.masontechnology.ie/x/Usercom_13.
- [20] Stanislav Kurajica,* Emilija Tkalcic, Gordana Matijašić, Lidija Ćurković, Zdravko Schauerl, Juraj Šipušić, and Vilko Mandić, "Influence of Agglomeration and Contamination in the Course of Amorphous Powder Grinding on Structure and Microstructure of Sintered Mullite", *CROATICA CHEMICA ACTA CCACAA*, ISSN 0011-1643, e-ISSN 1334-417X Croat. Chem. Acta 84 (1), 2011, 63–71. CCA-3450.
- [21] Jasper Chiguma, Edwin Johnson, Preyah Shah, Natalya Gornopolskaya, Wayne E. Jones Jr., "Thermal Diffusivity and Thermal Conductivity of Epoxy-Based Nanocomposites by the Laser Flash and Differential Scanning Calorimetry Techniques", *Open Journal of Composite Materials*, 3, July 2013, 51-62.

- [22] Roland T. Girard, Scotia, N.Y., assignor, "Beryllium Oxide-Organic Resin Composition", *United States Patent Office 3,310,520 Patented Mar. 21, 1967*.
- [23] Sanjeev Sharma, Jayashree Bijwe and Mukesh Kumar, "Comparison Between Nano and Micro-Sized Copper Particles as Fillers in NAO Friction Materials", *Nanomater. Nanotechnol.*, Vol. 3, Art. 12:2013, 2013, pp 1-9.
- [24] I. Tavman, Y. Aydogdu, M. Kk, A. Turgut, A. Ezan, "Measurement of heat capacity and thermal conductivity of HDPE/expanded graphite nanocomposites by differential scanning calorimetry", *Archives of Material Science and Engineering*, Volume 50, Issue 1, July 2011, pp 56-60.
- [25] Gyaneshwar Tandon, "Composite, Hybrid, and Multifunctional Materials, Volume 4: Proceedings of the 2014 Annual Conference on Experimental and Applied Mechanics", *Conference Proceedings of the Society for Experimental Mechanics Series, Springer*, 2014, pp 155-156.
- [26] Garrett, K.W.; Rosenberg, H.M., "The thermal conductivity of epoxy resin/powder composite materials". *J. Phys. D Appl. Phys.*, 7, 1974, 1247-1258.
- [27] P. Jakubowska, M. Osinska-Broniarz, A. Martyła, B. Sztorch, A. Sierczynska, M. Kopczyk, R. Przekop, "Thermal Properties Of Pp-Sio2 Composites Filled With Stber Silica", *Polish Society of Composite Materials*, 16: 3, 2016, 161-166.
- [28] Sung Min Ha, O Hwan Kwon, Yu Gyeong Oh, Yong Seok Kim, Sung-Goo Lee, Jong Chan Won, Kwang Soo Cho, Byoung Gak Kim and Youngjae Yoo, "Thermally conductive polyamide 6/carbon filler composites based on a hybrid filler system", *Sci. Technol. Adv. Mater.* 2015, 16, 065001 (10pp), doi:10.1088/1468-6996/16/6/065001.
- [29] P. S. Gaal, M. Thermitus and D. E. Stroe, "Thermal Con- ductivity Measurements Using the Flash Method," *Jour- nal of Thermal Analysis and Calorimetry*, Vol. 78, No. 1, 2004, pp. 185-189. doi:10.1023/B:JTAN.0000042166.64587.33.